DOE/ET-53088-298 IFSR #298

Stability of Low-Shear Tokamaks

F. L. Waelbroeck and *R. D. Hazeltine*
Institute for Fusion Studies
The University of Texas at Austin
Austin, Texas 78712

September 1987

Stability of Low-Shear Tokamaks

F. L. WAELBROECK and R. D. HAZELTINE
Institute for Fusion Studies
The University of Texas at Austin
Austin, Texas 78712

Abstract

It has been suggested that the recently observed fast sawtooth crashes are caused by a low-shear, pressure-driven ideal instability. This hypothesis is investigated, using asymptotic methods to solve the toroidal mode equations for a class of equilibria characterized by a low-shear central region in which $q - 1$ is small, separated from the wall by a region with finite shear. A dispersion relation which differs significantly from previous results is obtained. An explicit expression for the growth rate is given for a model q profile.

I. Introduction

The appropriateness of the Kadomtsev reconnection model for the description of the disruptive phase of sawtooth oscillations has been challenged by observations on JET.[1] First, the sawtooth collapses are too rapid to be accounted for on the basis of this model; furthermore, the observed flow is characterized by a cellular convection pattern, as opposed to the rigid displacement predicted by conventional kink-tearing mode theory.

Wesson has suggested that these observations could be explained, assuming a low-shear central region, by an ideal quasi-interchange mode with poloidal mode number $m = 1$.[2,3] Elementary considerations based on the cylindrical tokamak model and the toroidal stability analysis of Bussac et al.[4,5] lend support to this thesis. However, the cylindrical model cannot be relied on to draw conclusions regarding fixed-boundary instabilities in tokamaks.[6] The finite-shear analysis of Bussac et al. is also inadequate for the small values of shear and $|q-1|$ needed to allow instability at the observed values of the pressure gradient. Here q is the tokamak safety factor.

In this article we investigate the stability of Shafranov equilibria containing a central region with low shear and $q \simeq 1$. After reviewing the cylindrical results, we develop in Sec. II the general second-order energy expansion for arbitrary shear and discuss the various limiting cases. In Sec. III we solve the mode equations and derive the dispersion relation for the low-shear quasi-interchange mode.

II. Cylindrical Model

The difference between the kink instability for a sheared equilibrium and the corresponding quasi-interchange instability of low shear equilibria can be illustrated by the cylindrical tokamak model. The potential energy per unit length of a perturbation with poloidal mode number m and toroidal wavelength $k_z = n/R_0$ can be expanded for large wavelengths

$(\epsilon = k_z a \ll 1)$ as

$$\delta W = \delta W_0 + \epsilon^2 \delta W_2 + O\left(\epsilon^4\right), \tag{1}$$

$$\delta W_0 = \pi \int r\, dr \frac{(\vec{k}\cdot\vec{B})^2}{m^2} \left\{ r^2 \left(\frac{d\xi}{dr}\right)^2 + \left(m^2 - 1\right)\xi^2 \right\}, \tag{2}$$

where

$$(\vec{k}\cdot\vec{B}) = k_z B_z (m\mu - 1), \qquad \mu = \frac{B_\theta}{k_z r B_z} = \frac{1}{nq}. \tag{3}$$

The lowest order term in the expansion, δW_0, is non-negative, reflecting the stabilizing effect of field-line bending. Instability requires $(m\mu - 1) \sim \epsilon$ somewhere within the plasma. For sheared equilibria, such that $r\frac{d\mu}{dr} \sim 1$, this can only occur in a singular layer of width $\delta \sim \epsilon/\mu'$ (Fig. 1). The $m = 1$ mode is then constrained by the line-bending term to take the form of a rigid displacement, with the return flow taking place in the singular layer. This is the conventional $m = 1$ kink instability.[7] The $m \neq 1$ modes are strongly stabilized.

As the shear is reduced, however, the layer width grows until it eventually includes the entire core (Fig. 2). In the resulting low-shear $|m\mu - 1| \ll 1$ region the line bending energy is of the same order as the ϵ^2-order pressure-gradient driving term. The "quasi-interchange" instabilities associated with such equilibria will thus have continuous eigen-displacements distinct from the rigid displacement characteristic of the kink mode. The $m \neq 1$ modes are no longer strongly stabilized but the $m = 1$ mode will always be the first to reach criticality.[8]

The cylindrical mode equation can be solved in the case of a parabolic pressure profile $(p = p_0 \cdot [1 - (r/a)^2])$ and a constant q profile $(q = q_0)$.[9] Assuming $\epsilon \ll 1$, $\beta = \frac{p_0}{B_0^2} \sim \epsilon^2$, $\mu_0 = 1/nq_0$ such that $|m\mu_0 - 1| \ll 1$, one finds that

$$\xi_r(r) = \frac{1}{r} J_m(\kappa r/a) \tag{4}$$

$$\kappa^2 = 4\frac{k_z^2 a^2}{m^2} \frac{\beta_p + (m\mu_0 - 1)}{\hat{\gamma}^2 + (m\mu_0 - 1)^2}, \tag{5}$$

where J_m is the mth Bessel function, $\hat{\gamma}$ is the normalized growth rate

$$\hat{\gamma} = \gamma \tau_A, \qquad \tau_A = (k_z v_A)^{-1},$$

and $\beta_p = \frac{p_0}{B_{\theta a}^2}$, $B_{\theta a} = B_\theta(a)$ where a is the wall radius. The growth rate is determined by imposing appropriate boundary conditions. We consider two cases:

(i) q is constant throughout the plasma. The boundary condition is then $\xi(a) = 0$.

(ii) The constant q region is separated from the wall by a sheared region. In the sheared region the mode equation can be written

$$\frac{d}{dr}\left\{(m\mu - 1)^2 r^3 \frac{d\xi}{dr}\right\} - \left(m^2 - 1\right)(m\mu - 1)^2 r\xi = O\left(\epsilon^2\right). \tag{6}$$

The displacement must satisfy $\xi(a) = 0$ and must remain of order one as $(m\mu - 1) \rightarrow \epsilon$ in the low shear region. It is generally not possible to satisfy both conditions simultaneously in the lowest order due to the singularity in the mode equation for $m\mu - 1 = 0$. We therefore conclude that $\xi(r) \sim \epsilon^2$ in the sheared region. Assuming that the transition between the constant-q region and the sheared region is sharp, we may then deduce the growth rate by imposing the boundary condition $\xi(r_1) = 0$, where r_1 is the transition radius.

The growth rate for both of these cases can be written

$$\hat{\gamma}^2 = \frac{4k_z^2 \tilde{r}^2}{j_{m,n_r}^2 m^2}\left[\beta_p + (m\mu_0 - 1)\right] - (m\mu_0 - 1)^2, \tag{7}$$

where $\tilde{r} = a$ in Case (i) and $\tilde{r} = r_1$ in Case (ii). Here j_{m,n_r} is the n_rth radial node of the Bessel function $J_m(r)$.

$$J_m\left(j_{m,n_r}\right) = 0, \qquad j_{1,1} = 3.83\ .$$

We emphasize that these results are for a compressible plasma.[9] The various terms can be identified as the pressure-gradient driving term, a parallel current driving term, and the stabilizing line-bending term. We can distinguish two possible orderings for β_p and $(m\mu_0 - 1)$;

(i) For $\beta_p \sim 1$ and $(m\mu_0 - 1) \sim \epsilon$ the current driving term in the bracket can be neglected. The growth rate will be of order ϵ, as distinguished from the kink mode growth rate which is of order ϵ^2.

(ii) For $\beta_p \sim \epsilon^2$ and $(m\mu_0 - 1) \sim \epsilon^2$ there will be a stabilizing contribution from the parallel current term for $q_0 > m/n$. As we will see, the sign of this term is reversed in toroidal geometry.

III. Toroidal Analysis

We now turn to the question of the stability of large aspect-ratio, low-beta tokamaks with circular cross-sections. Toroidicity will weakly couple each poloidal harmonic to its neighboring $m \pm 1$ sidebands. In this section we restrict our analysis to modes dominated by the $m = 1$ poloidal harmonic and derive the appropriate mode equations for general q profiles. We will depart from a previous derivation of these equations[10] by working in flux coordinates. The resulting equations are easier to analyze, particularly in the low shear limit.

We define the equilibrium quantities as in Ref. 4 by $\vec{B} = \vec{\nabla}\varphi \times \vec{\nabla}F + T(F)\vec{\nabla}\varphi$, where φ is the azimuthal angle. The flux-based coordinate system is then defined by

$$\vec{B} \cdot \vec{\nabla} = \frac{T}{R^2}\left(\frac{1}{q}\frac{\partial}{\partial\theta} + \frac{\partial}{\partial\varphi}\right), \qquad d\tau = \frac{R^2}{R_0} r\, dr\, d\theta\, d\varphi. \tag{8}$$

The fluid displacement $\vec{\xi}$ is decomposed as follows: $\vec{\xi} = \vec{\xi}_p + \xi_{||}\vec{B}/B$ such that $\vec{\xi}_p \cdot \vec{\nabla}\varphi = 0$, $\xi_r = (T/T_0)\, \vec{\xi}_p \cdot \vec{\nabla} r$ and $\xi_\theta = (T/T_0)\, \vec{\xi}_p \cdot r\vec{\nabla}\theta$. The total energy of the perturbation can now be written

$$E = \delta W_a + \delta W_b + \delta W_d + \hat{\gamma}^2 N \tag{9}$$

where

$$N = \frac{n^2 B_0^2}{2R_0^2}\int \hat{\rho}|\vec{\xi}|^2 d\tau, \qquad \hat{\rho} = \frac{\rho}{\rho_0} \tag{10}$$

$$\delta W_d = \frac{1}{2}\int \Gamma p \left|\vec{\nabla}\cdot\vec{\xi}_p + \vec{B}\cdot\vec{\nabla}\left(\frac{\xi_{\|}}{B}\right)\right|^2 d\tau \tag{11}$$

$$\delta W_a = \frac{1}{2}B_0^2 R_0 \int r\, dr\, d\theta\, d\varphi \left|\frac{1}{r}\frac{\partial (r\xi_r)}{\partial r} + \frac{1}{r}\frac{\partial \xi_\theta}{\partial \theta}\right|^2 \tag{12}$$

$$\begin{aligned}\delta W_b = {} & \frac{1}{2}\frac{B_0^2}{R_0}\int r\, dr\, d\theta\, d\varphi \Bigg\{ \left| r\vec{\nabla}\theta\left(\frac{\partial \xi_r}{\partial\varphi} + \frac{1}{q}\frac{\partial \xi_r}{\partial \theta}\right) + \vec{\nabla}r\left(\frac{\partial}{\partial r}\left(\frac{r\xi_r}{q}\right) - \frac{\partial \xi_\theta}{\partial \varphi}\right)\right|^2 \\ & + R_0\frac{dT}{dF}\left[|\xi_r|^2 r\frac{d}{dr}\left(\frac{1}{q}\right) + \xi_\theta\left(\frac{\partial}{\partial\varphi} + \frac{1}{q}\frac{\partial}{\partial\theta}\right)\xi_r^* + \xi_\theta^*\left(\frac{\partial}{\partial\varphi} + \frac{1}{q}\frac{\partial}{\partial\theta}\right)\xi_r\right] \\ & + R_0\frac{dP}{dF}\left[\frac{1}{r}\frac{\partial}{\partial r}\left(\frac{R^2|\xi_r|^2 r^2}{qT}\right) + \frac{R^2}{T}\left(\xi_\theta\frac{\partial \xi_r^*}{\partial\varphi} + \xi_\theta^*\frac{\partial \xi_r}{\partial \varphi}\right)\right]\Bigg\}.\end{aligned} \tag{13}$$

Here $B_0 = T_0/R_0$ and Γ is the ratio of specific heats. The large aspect-ratio expansion of the energy can be obtained by straightforward expansion of the coefficients in these expressions. We define ϵ by $\epsilon = na/R_0$ so that the cylindrical model may be recovered by taking the limit $n \to \infty$, $\epsilon \to k_z a$. The major radius is given by[11]

$$R = R_0\left\{1 - \frac{\epsilon}{n}\rho_0\cos\omega_0 - \left(\frac{\epsilon}{n}\right)^2\delta(r)\right\}, \tag{14}$$

$$\rho_0 = r + \left(\frac{\epsilon}{n}\right)^2[\eta(r) + \nu(r)\cos 2\theta] + O\left(\frac{\epsilon}{n}\right)^3 \tag{15}$$

$$\omega_0 = \theta + \frac{\epsilon}{n}\lambda(r)\sin\theta + \left(\frac{\epsilon}{n}\right)^2\mu(r)\sin 2\theta + O\left(\frac{\epsilon}{n}\right)^3, \tag{16}$$

where we have rescaled $r : r/a \to r$. The coefficient $\delta(r)$ describes the eccentricity of the (nearly circular) flux surfaces. Applying the definitions (8) one finds

$$\lambda(r) = -\left(\frac{d\delta}{dr} + r\right), \tag{17}$$

$$\eta(r) = -\frac{r}{2}\left(\delta + \frac{r^2}{4}\right). \tag{18}$$

The $m = 2$, ϵ^2-order coefficients $\nu(r)$ and $\mu(r)$ will not be needed. $\delta(r)$ is given by the equilibrium (Grad-Shafranov) equation:

$$\frac{d\delta(r)}{dr} \equiv \alpha(r) = \left(\beta_p(r) + \frac{1}{2} l_i(r)\right) \cdot r, \tag{19}$$

where

$$\beta_p(r) = -\frac{2R_0^2 q^2}{B_0^2 r^4} \int_0^r \hat{r}^2 \frac{dp(\hat{r})}{d\hat{r}} d\hat{r}, \tag{20}$$

$$l_i(r) = \frac{2q^2}{r^4} \int_0^r \frac{\hat{r}^3}{q^2(\hat{r})} d\hat{r}. \tag{21}$$

The following geometrical quantities are also needed:

$$(\bar{\nabla} r)^2 = 1 - 2\left(\frac{\epsilon}{n}\right) \alpha \cos\theta + \left(\frac{\epsilon}{n}\right)^2 \left[\frac{1}{2}\alpha^2 + \frac{3}{4} r^2 + \delta\right], \tag{22}$$

$$\begin{aligned}(r\vec{\nabla}\theta)^2 &= 1 + 2\left(\frac{\epsilon}{n}\right)(\alpha + r)\cos\theta \\ &+ \left(\frac{\epsilon}{n}\right)^2 \left[2\alpha^2 + 4r\alpha + \frac{9}{4}r^2 + \frac{1}{2}r^2\alpha'^2 + r\alpha'\alpha + r^2\alpha' + \delta\right],\end{aligned} \tag{23}$$

$$(r\bar{\nabla}\theta \cdot \bar{\nabla} r) = \left(\frac{\epsilon}{n}\right) [r\alpha' + \alpha + r] \sin\theta. \tag{24}$$

Now the energy can be expressed as

$$E = \epsilon^{-2}\delta W_a + \delta W_0 + \hat{\gamma}^2 N_0 + \frac{\epsilon}{n}\delta W_{1T} + \epsilon^2 \left(\delta W_{2C} + \frac{1}{n^2}\delta W_{2T}\right). \tag{25}$$

We next substitute the expansion

$$\xi = \sum_{k=0}^{\infty} \sum_m \epsilon^k \xi_m^{(k)}(r) \exp\{i(m\theta - n\varphi)\} \tag{26}$$

into (25) and minimize order by order. In the lowest orders, ϵ^{-2} and ϵ^0, we recover the familiar cylindrical results

$$\frac{d}{dr}\left(r\xi_{rm}^{(k)}\right) + im\xi_{\theta m}^{(k)} = 0, \qquad k = 0, 1, \forall m \tag{27}$$

and

$$\delta W_0 = \frac{n^2 B_0^2}{2R_0} \int r\, dr (\mu - 1)^2 \left(r \frac{d\xi_{r1}^{(0)}}{dr}\right)^2, \tag{28}$$

where $\mu = \frac{1}{nq}$. The identity of the energy expansions for cylindrical and toroidal geometries up to this order justifies the use of the cylindrical model to draw conclusions as to the nature of the possible instabilities. In particular the conclusion that the unstable modes are characterized by rigid shift displacements for sheared equilibria and cellular convection flows within low shear regions is also valid in toroidal geometry. However, at this order the appropriate displacements are only marginally stable: stability is ultimately determined by the ϵ^2-term in the energy expansion. This implies that $\hat{\gamma}$ is at most of order ϵ.

After eliminating $\xi_{\theta 1}^{(0)}$, $\xi_{\theta 2}^{(1)}$, and $\xi_{r0}^{(1)}$ with Eq. (27), the ϵ^2-order term can be expressed as a functional of $\xi_{r1}^{(0)}$, $\xi_{\theta 0}^{(1)}$, $\xi_{r2}^{(1)}$, $\xi_{\theta 1}^{(2)}$, $\xi_{\|0}^{(0)}$, and $\xi_{\|2}^{(0)}$. All of these variables except $\xi_{r1}^{(0)}$ and $\xi_{r2}^{(1)}$ can be eliminated through algebraic minimizations. The results are:

$$-in\xi_{\theta 0}^{(1)} = \alpha(\mu-1)r\frac{d\xi_{r1}^{(0)}}{dr} - \left\{\frac{1}{2}(r\alpha' + 3\alpha + r) - r\mu\right\}\xi_{r1}^{(0)} \tag{29}$$

$$\begin{aligned} -i\xi_{\theta 1}^{(2)} &= -r^2\frac{d}{dr}\left[(\mu-1)r\xi_{r1}^{(0)}\right] - r\left(r^2\mu\right)'(\mu-1)\xi_{r1}^{(0)} \\ &\quad + \frac{1}{2}\mu^2\left[r\alpha' + \left(3 + 2r\frac{\mu'}{\mu}\right)\alpha - r\right]r\xi_{r1}^{(0)} \end{aligned} \tag{30}$$

$$-in\xi_{\|0}^{(0)} = \frac{\Gamma\beta}{\hat{\rho}\hat{\gamma}^2 + \Gamma\beta}\left\{\xi_{r1}^{(0)} + \frac{d}{dr}\left(r\xi_{r1}^{(0)}\right)\right\} \tag{31a}$$

$$-in\xi_{\|2}^{(0)} = \frac{\Gamma\beta(2\mu-1)}{\hat{\rho}\hat{\gamma}^2 + \Gamma\beta(2\mu-1)^2}\left\{\xi_{r1}^{(0)} - \frac{d}{dr}\left(r\xi_{r1}^{(0)}\right)\right\}, \tag{31b}$$

where $\beta = p/B_0^2$. Minimization with respect to the remaining two variables finally yields the two coupled second order differential equations.[10]

$$\left[\epsilon^{-2}\left(L_1 + T\right) - G_1^{(2)}\right]\xi_{r1}^{(0)} = C^{(1)}\xi_{r2}^{(1)} \tag{32a}$$

$$L_2\xi_{r2}^{(1)} = C^{(1)\dagger}\xi_{r1}^{(0)}. \tag{32b}$$

Here the operators L_m are the line-bending operators, T is the kinetic energy operator, $C^{(1)}$ is the toroidal coupling operator, and G_1 is the driving term containing the cylindrical coefficient g_1 as well as toroidal corrections. $C^{(1)\dagger}$ is the operator adjoint to $C^{(1)}$, defined by

$$\int_0^1 dr\, f(r) C^{(1)} [g(r)] = \int_0^1 dr\, g(r) C^{(1)\dagger} [f(r)] \,. \tag{33}$$

Explicitly,

$$L_m \xi = \frac{d}{dr} \left\{ \left(\mu - \frac{1}{m} \right)^2 r^3 \frac{d\xi}{dr} \right\} - \left(m^2 - 1 \right) \left(\mu - \frac{1}{m} \right)^2 r\xi. \tag{34}$$

The general expression for $C^\dagger$ is

$$\begin{aligned} nC^\dagger \xi_1 &= \left(\mu - \frac{1}{2} \right) \alpha r^3 \frac{d}{dr} \left\{ (\mu - 1) \frac{d\xi_1}{dr} \right\} + \left\{ (\mu - 1) r \mu' \alpha \right. \\ &- \left. \frac{1}{2} \left(\mu - \frac{1}{2} \right) (\mu - 1)(r\alpha' - 3\alpha + 3r) - \frac{1}{4} \mu (r\alpha' + 3\alpha - r) \right\} r^2 \frac{d\xi_1}{dr} \\ &- \left\{ \left[\left(\mu - \frac{1}{2} \right)^2 r^3 \left(\alpha + \frac{r}{2} \right) \right]' - 3r \left(\mu - \frac{1}{2} \right)^2 \left(\alpha + \frac{r}{2} \right) \right\} \xi_1, \end{aligned} \tag{35}$$

where we note that the coefficient of ξ_1 is simply $-L_2(\alpha + r/2)$. For $q - 1 \sim \epsilon$, the kinetic energy operator can be written

$$T\xi_1 = \frac{d}{dr} \left\{ \hat{\rho} \hat{\gamma}^2 \zeta r^3 \frac{d\xi_1}{dr} \right\} + \hat{\gamma}^2 r^2 \frac{d}{dr} (\hat{\rho} \zeta) \xi_1, \tag{36}$$

where

$$\zeta = \frac{\hat{\rho} \hat{\gamma}^2 + (1 + 2n^{-2})\, \Gamma \beta}{\hat{\rho} \hat{\gamma}^2 + \Gamma \beta}.$$

When $\hat{\gamma}^2 \ll \Gamma\beta$, $\hat{\rho} = 1$, this expression reduces to

$$T\xi_1 = \frac{d}{dr} \left\{ \left(1 + \frac{2}{n^2} \right) \hat{\gamma}^2 r^3 \frac{d\xi_1}{dr} \right\}. \tag{37}$$

The operator G can be written

$$\begin{aligned} G &= \left(1 - \frac{1}{n^2} \right) G_C + \frac{1}{n^2} G_T, \qquad (38) \\ G_C \xi_1 &= \frac{d}{dr} \left\{ (\mu - 1)^2 r^5 \frac{d\xi_1}{dr} \right\} - \left\{ \left(\mu^2 r^4 \beta_p \right)' + (\mu - 1)(\mu + 3) r^3 \right\} \xi_1 \end{aligned}$$

$$+ \left\{\frac{r}{2}(\mu-1)^2\left(\mu^2 r^4\left(\beta_p-1\right)\right)'\right\}'\xi_1, \tag{39}$$

where the last (total derivative) coefficient of ξ_1 arises from our definition of $\xi_r = (T/T_0)\,\vec{\xi}\cdot\vec{\nabla}r$;

$$\begin{aligned} G_T\xi_1 &= \frac{d}{dr}\left\{(\mu-1)^2 u r^3 \frac{d\xi_1}{dr}\right\} + \left\{\left(\mu-\frac{1}{2}\right)^2 r\left[r^2\left(\alpha+\frac{r}{2}\right)'^2 + 3\left(\alpha+\frac{r}{2}\right)^2\right]\right. \\ &+ \left.\left(\mu^2-1\right)\frac{r^3}{2} + \frac{3}{4}\left(r^2\alpha^2 - r^3\alpha\right)'\right\}\xi_1 \\ &+ \left\{\frac{d}{dr}\left[(\mu-1)^2 r^2 v + \left(\mu^2-1\right)r^2 w\right]\right\}\xi_1, \end{aligned} \tag{40}$$

where

$$u = \frac{\alpha^2}{2} + \frac{1}{4}r^2 - \delta \tag{41}$$

$$v = \frac{1}{4}\left[3r\alpha\alpha' + 3\alpha^2 + 5r\alpha + 3r^2\right] + \frac{1}{2r}\left[\mu^2 r^4\left(\beta_p - 1\right)\right]' \tag{42}$$

$$w = \frac{1}{4}\left[r\alpha\alpha' + 3\alpha^2 - r\alpha\right]. \tag{43}$$

Three asymptotic cases can now be distinguished, according to the ordering of $q-1$ and $r\frac{dq}{dr}$:

(i) $r\frac{dq}{dr} \sim q-1 \sim 1$ except in a singular layer of width ϵ^2 where $q-1 \sim \epsilon^2$. This "finite shear" case was treated by Bussac et al.[4] for monotone q profiles and recently extended to more complicated profiles by Hastie et al.[12] The operators in Eqs. (35)–(43) have been written in such a way that one can easily recover these results.

(ii) $r\frac{dq}{dr} \sim q-1 \sim \epsilon$. In this "low shear" ordering we recover the equations of Ware and Haas.[13] The instability is pressure-driven, including the $j_{\|}$ contribution arising from the nonzero divergence of $j_{\perp}$ (Pfirsch-Schlüter current).[14]

(iii) $r\frac{dq}{dr} \sim q-1 \sim \epsilon^2$, $\beta_p \sim \epsilon$. For this "very low shear" ordering there appears an additional driving term due to the divergenceless part of $j_{\|}$.[14]

The *free boundary* stability problem for the "low shear" and "very low shear" cases was studied by Frieman et al.,[15] who corrected a small error in the coefficient of the current driving term reported in Ref. 14. Their analysis was restricted to constant q profiles. We present the first complete *fixed boundary* stability analysis of the "low shear" case for general q profiles.

IV. Solution of the Mode Equations

For the cases of low or very low shear the mode equations can be written

$$\frac{d}{dr}\left\{\epsilon^{-2}\left[(\mu-1)^2+\left(1+\frac{2}{n^2}\right)\hat{\gamma}^2\right]r^3\frac{d\xi_1}{dr}\right\}$$
$$+\left(1-\frac{1}{n^2}\right)\left\{\left(r\beta_p'+4\beta_p\right)+(\mu+3)(\mu-1)\right\}r^3\xi_1$$
$$-\frac{4}{n^2}\left\{\left(\frac{r}{4}\beta_p'+\beta_p\right)^2+\frac{13}{16}(\mu-1)\right\}r^3\xi_1=\frac{1}{n}\left(\frac{r}{4}\beta_p'+\beta_p\right)\frac{d}{dr}\left(r^3\xi_2\right) \quad (44a)$$

$$\frac{d}{dr}\left\{r^3\frac{d\xi_2}{dr}\right\}-3r\xi_2=-\frac{4}{n}r^3\frac{d}{dr}\left\{\left(\frac{r}{4}\beta_p'+\beta_p\right)\xi_1\right\}. \quad (44b)$$

We first remark that the cylindrical equations are recovered in the limit $n\to\infty$. Setting $n=1$ we integrate the second equation, assuming ξ_1 and ξ_2 are bounded at the origin:

$$\xi_2=r^{-3}\int_0^r\tilde{r}^4\beta_p(\tilde{r})\frac{d\xi_1(\tilde{r})}{d\tilde{r}}d\tilde{r}+\left[e-\beta_p(r)\xi_1(r)\right]\cdot r, \quad (45a)$$

where e is an integration constant. Thus (44a) becomes

$$\frac{d}{dr}\left\{\epsilon^{-2}\left[(\mu-1)^2+3\hat{\gamma}^2\right]r^3\frac{d\xi_1}{dr}\right\}-\frac{13}{4}(\mu-1)r^3\xi_1=\frac{d}{dr}\left\{er^4\beta_p\right\}. \quad (45b)$$

In order to determine e we now specialize to the moderately low shear case for which the current-driving term, proportional to $(\mu-1)$, can be dropped. Equation (45b) is then easily integrated:

$$\frac{d\xi_1}{dr}=\frac{\epsilon^2er\beta_p}{(\mu-1)^2+3\hat{\gamma}^2}. \quad (46)$$

As in the cylindrical case we now consider two possibilities for the boundary conditions. In the first case we assume that the low shear assumptions are satisfied throughout the entire plasma. The appropriate boundary conditions are then $\xi_1(1) = \xi_2(1) = 0$. This leads to

$$1 = -\int_0^1 \frac{r^5 \left(\epsilon\beta_p\right)^2}{3\hat{\gamma}^2 + (\mu - 1)^2} dr \tag{47}$$

which can only be satisfied by $\hat{\gamma}^2 < 0$. We conclude that in the absence of shear the mode is stable. This is due to the stabilizing influence of the $m = 2$ harmonic which is driven off-resonance by the $m = 1$ mode.

In the second case the low shear central region is separated from the wall by a sheared region. We will solve the mode equations by matching the solution in the inner (low shear) region to the solution in the outer (sheared) region. In practical terms this procedure can be expected to yield good results when the transition is sufficiently abrupt. In the sheared region $(\mu - 1) \sim 1$ but $\xi_1 \sim \epsilon^2$. Retaining terms of order ϵ^2, we obtain from (32b) the following outer equation for ξ_2:

$$L_2\xi_2 = \frac{d}{dr}\left\{\left(\mu - \frac{1}{2}\right)^2 r^3 \frac{d\xi_2}{dr}\right\} - 3\left(\mu - \frac{1}{2}\right)^2 r\xi_2 = 0. \tag{48}$$

With the boundary condition $\xi_2(1) = 0$ if $q(1) < 2$ or ξ_2 bounded as $r \to r_2$ for $q(r_2) = 2$. The asymptotic form of the solution to this equation in the low shear region is

$$\xi_2 \sim \left(\frac{r}{r_2}\right) + \sigma\left(\frac{r}{r_2}\right)^{-3}. \tag{49}$$

The constant σ is determined by integrating (48) through the outer region. The dispersion relation is now determined by matching this asymptotic solution to the corresponding asymptotic form of the inner region solution in the outer region:

$$\sigma = \left(\frac{r_2}{a}\right)^2 \int_0^a \frac{\left(\epsilon\beta_p(r)\right)^2}{3\hat{\gamma}^2 + (\mu - 1)^2} \left(\frac{r}{r_2}\right)^5 d\left(\frac{r}{r_2}\right), \tag{50}$$

where we have restored the dimensions. Note that the integrand becomes negligible in the sheared region. Equation (50), in which σ is implicitly determined by Eqs. (48) and (49), gives the general dispersion relation for the quasi-interchange instability at low shear.

To obtain an explicit dispersion relation, we use the model safety factor profile $\mu = \frac{1}{2} + \left(\mu_0 - \frac{1}{2}\right)\left[1 - (r/r_2)^{2\lambda}\right]$, for which Eq. (48) is a hypergeometric equation. When $r_2 < a$, the constant σ can be determined from the linear transformation formulas[16] between the fundamental solutions at the two singular points $r = 0$ and $r = r_2$, provided $\lambda > 2$. For large λ the result can be written

$$\sigma = \frac{1}{3}\left(1 - \frac{2}{\lambda}\right) \tag{51}$$

with an error less than 5% for $\lambda \geq 3$. In order to calculate the integral in Eq. (50) we use the pressure profile $p(r) = p_0\left[1 - (r/a)^{2\nu}\right]$. Near marginal stability $\left(\hat{\gamma}^2 \ll |\mu_0 - 1|^2\right)$, this integral can be evaluated asymptotically for $|\mu_0 - 1| \ll 1$. One finds

$$\hat{\gamma}^2 = E\left\{K\left(\epsilon\beta_{p1}\right)^2 - (\mu_0 - 1)^2\right\} + O\left[(\mu_0 - 1)^{4-\zeta}\right], \tag{52}$$

where

$$K = \frac{1}{2\sigma(2\nu + 1)}\left(\frac{r_1}{a}\right)^2\left(\frac{r_1}{r_2}\right)^4\frac{(\pi\zeta)(1 - \zeta)}{\sin(\pi\zeta)} \tag{53}$$

$$E = \left[3(1 - \zeta/3)(1 - \zeta/2)\right]^{-1} \tag{54}$$

$$\zeta = (2\nu + 1)/\lambda$$

$$r_1 = r_2\left(\frac{1 - \mu_0}{\mu_0 - \frac{1}{2}}\right)^{1/2\lambda}$$

$$\beta_{p1} = \beta_p\left(r_1\right).$$

Equation (52) is in good agreement with numerical results,[17,18] allowing for corrections related to the current-driving term. An estimate of the error made in neglecting that term can be obtained from the zero pressure, constant q solution[15]: $\xi_r = \frac{1}{r}J_1(\kappa r)$ with $\kappa^2 = -\frac{13}{4}\epsilon^2(\mu - 1)\left[3\hat{\gamma}^2 + (\mu - 1)^2\right]^{-1}$. Taking $\xi\left(r_1\right) = 0$, one finds $\hat{\gamma}^2 = (\mu - 1)\left(\mu_c - \mu\right)$, where $\mu_c = 1 - \frac{13}{4}\frac{\epsilon^2}{j_{1,1}^2}\left(\frac{r_1}{a}\right)^2$. The current term is thus destabilizing for $q > 1$.

We emphasize that Eqs. (52)–(54) apply only to nearly marginal conditions. However, for the particular case $\mu_0 = 1$, our model profile also allows a calculation of the growth rate far from marginality. By integrating Eq. (50) in this case one finds

$$\hat{\gamma}^2 = \frac{1}{12}\left[\frac{2}{\sigma(2\nu+1)}\left(\frac{r_2}{a}\right)^2 (\epsilon\beta_{p2})^2 \frac{\pi}{2}\zeta \csc\left(\frac{\pi}{2}\zeta\right)\right]^{\frac{1}{1-\zeta/2}}, \tag{55}$$

where $\beta_{p2} \equiv \beta_p(r_2)$. Thus, in the flat current profile limit ($\lambda \gg \nu$), the growth rate scaling is similar to that near marginal stability $\left(\hat{\gamma}^2 \sim (\epsilon\beta_{p2})^2\right)$. However, for more rounded current profiles ($\zeta \lesssim 1$) we find a different scaling, leading to a reduced growth rate away from marginal stability (e.g., for $\lambda = 3$, $\nu = 1$, $\hat{\gamma} \sim (\epsilon\beta_{p2})^2$).

We conclude this section by looking at the "low-shear" $n \neq 1$ modes. Although these modes remain stable when the $m = n = 1$ mode reaches criticality, they will be important during the nonlinear development of the instability. The mode equations for general m, n are[13,15]:

$$\begin{aligned}
\epsilon^{-2}(L_m + T_m)\xi_m &- \frac{1}{n^2m^2}\left\{\frac{1}{2}\left(r\beta_p' + 4\beta_p\right)^2 + \left(1 - \frac{n^2}{m^2}\right)\left(r\beta_p' + 4\beta_p\right)\right\} r^3\xi_m \\
&= \frac{1}{2nm^2(1\pm m)} r^{1\mp m}\left(r\beta_p' + 4\beta_p\right)\frac{d}{dr}\left(r^{2\pm m}\xi_{m\pm1}\right) \qquad (56a)\\
L_{m\pm1}\xi_{m\pm1} &= \frac{1}{m^2(1\pm m)^2}\left\{\frac{d}{dr}\left(r^3\frac{d\xi_{m\pm1}}{dr}\right) - \left[(m\pm1)^2 - 1\right] r\xi_{m\pm1}\right\} \\
&= -\frac{1}{2nm^2(1\pm m)} r^{2\pm m}\frac{d}{dr}\left\{\left(r\beta_p' + 4\beta_p\right) r^{1\mp m}\xi_m\right\}. \qquad (56b)
\end{aligned}$$

The sideband equations may again be integrated:

$$n\xi_{m\pm1} = -\frac{1}{2}(1\pm m) r^{-(2\pm m)}\int_0^r d\hat{r}\left(\hat{r}\beta_p' + 4\beta_p\right)\hat{r}^{2\pm m}\xi_m + e_{\pm} r^{m\pm1-1}, \tag{57a}$$

leaving a decoupled main-harmonic equation:

$$\frac{d}{dr}\left\{\left[\left(1 + 2\frac{m^2}{n^2}\right)\frac{\hat{\gamma}^2}{m^2} + \left(\mu - \frac{1}{m}\right)^2\right] r^3\frac{d\xi_m}{dr}\right\}$$

$$-\left(m^2-1\right)\left[\left(1+2\frac{m^2}{n^2}\right)\frac{\hat{\gamma}^2}{m^2}+\left(\mu-\frac{1}{m}\right)^2\right]r\xi_m$$

$$-\frac{\epsilon^2}{n^2m^2}\left(1-\frac{n^2}{m^2}\right)\frac{d}{dr}\left(r^4\beta_p\right)\xi_m=\frac{\epsilon^2}{n^2}\frac{e_+}{m^2}\frac{d}{dr}\left(r^4\beta_p\right)r^{m-1}. \qquad (57b)$$

We solve Eq. (57b) for constant $\mu=\mu_0\simeq 1$, $m=n$, and $\beta_p=\beta_0 r^{2\nu-2}$. After imposing the boundary condition $\xi_m(r_1)=0$ at the transition radius r_1 between the low-shear and finite-shear regions, one finds

$$\xi_m(r)=\left(\frac{\epsilon}{n}\right)^2\frac{\nu+1}{2\nu(\nu+m)}\frac{e_+\beta_0}{3\hat{\gamma}^2+\left(\frac{1}{q}-1\right)^2}\left(r^{2\nu}-r_1^{2\nu}\right)r^{m-1}. \qquad (58)$$

The dispersion relation is then obtained by matching the solution for ξ_{m+1} given in (57a) to the low-shear limit of the outer equations:

$$\xi_{m+1}(r)\sim\left(\frac{r}{r_2}\right)^m+\sigma_m\left(\frac{r}{r_2}\right)^{-(2+m)}. \qquad (59)$$

We find

$$\hat{\gamma}^2=E\left[K_m\left(\frac{\epsilon}{n}\beta_p\right)^2-\left(\frac{1}{q_0}-1\right)^2\right], \qquad (60)$$

where $E=1/3$,

$$K_m=\frac{1}{4\sigma_m}\frac{(\nu+1)^2(1+m)}{(\nu+m)^2(2\nu+m)}\left(\frac{r_1}{r_2}\right)^{2m+2}\left(\frac{r_1}{a}\right)^2. \qquad (61)$$

The value of σ_m calculated for our model q profile is

$$\sigma_m=\frac{m}{m+2}\left[1-\frac{m+1}{\lambda}+O\left(\frac{1}{\lambda^2}\right)\right]. \qquad (62)$$

From the large m behavior of K_m,

$$K_m\sim m^{-2}\exp\left\{-2m\left|\ln\left(\frac{r_1}{r_2}\right)\right|\right\}$$

we see that the growth rate at resonance ($q_0=1$) for toroidal geometry will decrease much faster for large values of m than the corresponding cylindrical result. We note that the presence of the sheared region is also necessary for instability with $n\neq 1$.

V. Conclusion

We have re-examined the stability of $m = 1$ modes in a low-beta tokamak, allowing for relatively weak magnetic shear. Our formalism is sufficiently general to allow previous results[4,5,12–15] to be recovered in appropriate limits. However, in the weak shear, $|q-1| \ll 1$ case we obtain a novel growth rate, given in general by Eq. (50), and more explicitly, for a model profile, by Eq. (52). The new quasi-interchange instability displays no threshold with regard to the poloidal beta. The scaling of its growth rate ($\hat{\gamma} \sim \epsilon\beta_p$ for flat current profiles) and its continuous, cellular-convection type of flow set it sharply apart from the usual kink mode $\left(\hat{\gamma} \sim (\epsilon\beta_p)^2\right)$. The quasi-interchange mode does, nonetheless, share some features with the kink mode, such as a sensitivity to the location of the $q = 2$ surface. Our analysis differs in this respect from that of Ramos[19] for noncircular tokamaks in which the sidebands as well as the principal harmonic were assumed to vanish outside the low-shear region. Numerical results for the noncircular case have also been obtained by Turnbull.[20]

The nature of the marginal stability condition is, however, the most important characteristic of this model. Indeed, by requiring the pressure gradient to balance the line-bending force at marginal stability, we have taken a significant step away from the traditional emphasis on q profiles to determine critical stability. This trait distinguishes this model from that of Denton et al.,[19] which is also based on a low-shear central region but which relies on the line-bending term in a surrounding island to drive the instability. In Wesson's model,[2] therefore, the evolution of the pressure profile during the rise phase of the sawtooth becomes as important as the current diffusion. In particular, it is not clear in this model why additional heating fails to shorten the sawtooth period. Another area for concern is the failure of the theory to account for the suddenness of the onset of the instability. It is hoped that this feature can be accounted for by a nonlinear analysis. In this respect we have found that the linearized Reduced Magnetohydrodynamics equations[20] are identical to the full Magnetohydrodynamics equations in the ordering of Ware and Haas, except for the neglect of parallel kinetic energy and the effects of compressibility.

After this work was completed we learned of a similar analysis by Hastie and Hender, in which equivalent marginal stability criteria were obtained.[23]

Acknowledgements

We wish to thank Dr. A. Y. Aydemir for many helpful discussions and W. Miner for help with the figures. We also benefitted from comments by R. Denton. This research was supported by the U. S. Department of Energy Contract No. DE-FG05-80ET-53088.

References

1. A. W. Edwards, D. J. Campbell, W. W. Engelhardt, H. V. Fahrbach, R. D. Gill, R. S. Granetz, S. Tsuji, B. J. D. Tubbing, A. Weller, J. Wesson, and D. Zasche, Phys. Rev. Lett. **57**, 210 (1986).

2. J. A. Wesson, Plasma Physics and Controlled Fusion **28**, 243 (1986).

3. J. A. Wesson, P. Kirby, and M. F. F. Nave, in **Plasma Physics and Controlled Nuclear Fusion Research 1986**, Kyoto, Japan, 1986 (IAEA, Vienna, 1987), Vol. 2, p. 3.

4. M. N. Bussac, R. Pellat, D. Edery, and J. L. Soulé, Phys. Rev. Lett. **35**, 1638 (1975).

5. L. E. Zakharov, Fiz. Plasmy **4**, 898 (1978) [Sov. J. Plasma Phys. **4**, 503 (1979)].

6. V. D. Shafranov, Zh. Tekh. Fiz. **40**, 241 (1970) [Sov. Phys. Tech. Phys. **15**, 175 (1970)].

7. M. N. Rosenbluth, R. Y. Dagazian, and P. H. Rutherford, Phys. Fluids **16**, 1894 (1973).

8. W. A. Newcomb, Ann. Phys. **10**, 232 (1960).

9. J. P. Goedbloed and H. J. L. Hagebeuk, Phys. Fluids **15**, 1090 (1972).

10. G. B. Crew and J. J. Ramos, Phys. Fluids **26**, 2621 (1983).

11. V. D. Shafranov and E. I. Yurchenko, Soviet Physics JETP **26**, 682 (1968).

12. R. J. Hastie, T. C. Hender, B. A. Carreras, L. A. Charlton, and J. A. Holmes, Phys. Fluids **30**, 1756 (1987).

13. A. A. Ware and F. A. Haas, Phys. Fluids **9**, 956 (1966).

14. A. A. Ware, Phys. Rev. Lett. **26**, 1304 (1971).

15. E. A. Frieman, J. M. Green, J. L. Johnson, and K. E. Weimer, Phys. Fluids **16**, 1108 (1973).

16. M. S. Abramowitz and I. A. Stegun, **Handbook of Mathematical Functions**, (Dover, New York, 1972).

17. A. Y. A. Aydemir, Phys. Rev. Lett. **59**, 649 (1987).

18. J. A. Holmes, B. A. Carreras, L. A. Charlton, and V. E. Lynch, Bull. Am. Phys. Soc. **32**, 1772 (1987).

19. J. J. Ramos, Bull. Am. Phys. Soc. **32**, 1738 (1987).

20. A. D. Turnbull, Bull. Am. Phys. Soc. **32**, 1738 (1987).

21. R. G. Kleva, J. F. Drake, and R. E. Denton, Phys. Fluids **30**, 2119 (1987).

22. H. R. Strauss, Phys. Fluids **20**, 1354 (1977).

23. R. J. Hastie, T. C. Hender, private communication.

Figure Captions

1. Radial eigendisplacement for a q-profile with $q' \sim 1$ at the rational surface $r = r_s$, where $q(r_s) = 1$.

2. Radial eigendisplacement for a q-profile with a low shear central region such that $|q - 1| \sim \epsilon$.

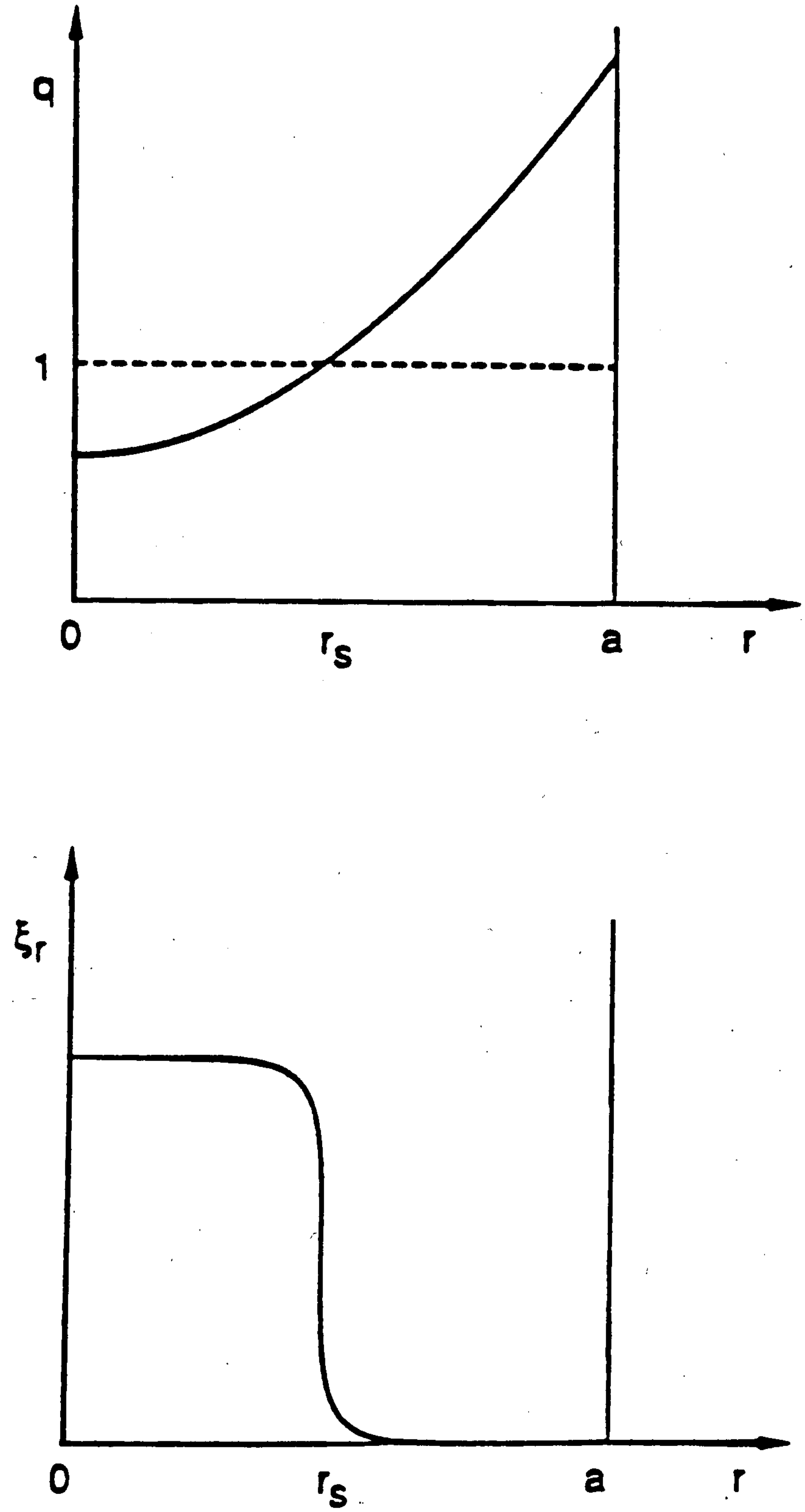

Fig. 1

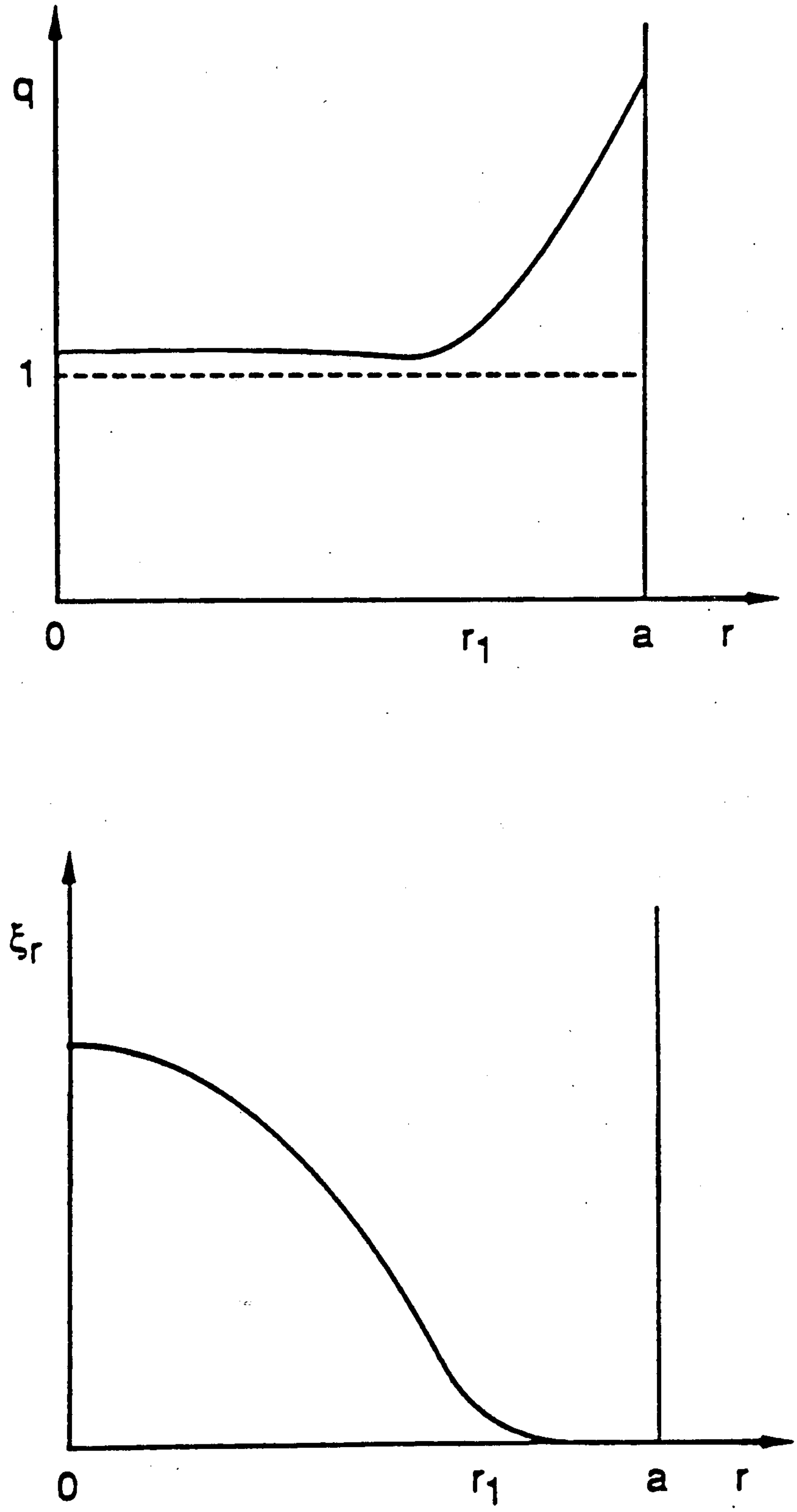

Fig. 2